## PAPER

Check for updates

# Development of optical sensor for water in acetonitrile based on propeller-structured BODIPY-type pyridine–boron trifluoride complex†

Shuhei Tsumura, Kazuki Ohira, Keiichi Imato [ID] * and Yousuke Ooyama [ID] *

A propeller-structured 3,5,8-trithienyl-BODIPY-type pyridine–boron trifluoride complex, **ST-3-BF₃**, which has three units of 2-(pyridin-4-yl)-3-(thiophen-2-yl)acrylonitrile at the 3-, 5-, and 8-positions on the BODIPY skeleton, was designed and developed as an intramolecular charge transfer (ICT)-type optical sensor for the detection of a trace amount of water in acetonitrile. The characterization of **ST-3-BF₃** was successfully determined by FTIR, $^1$H and $^{11}$B NMR measurements, high-resolution mass spectrometry (HRMS) analysis, thermogravimetry-differential thermal analysis (TG-DTA), photoabsorption and fluorescence spectral measurements, and density functional theory (DFT) calculations. **ST-3-BF₃** showed a broad photoabsorption band in the range of 600 to 800 nm, which is assigned to the $S_0 \rightarrow S_1$ transition of the BODIPY skeleton with the expanded π-conjugated system over the 2-(pyridin-4-yl)-3-(thiophen-2-yl)acrylonitrile units at the 3-, 5-, and 8-positions onto the BODIPY core. In addition, a photoabsorption band was also observed in the range of 300 to 550 nm, which can be assigned to the ICT band between the 2-(pyridin-4-yl)-3-(thiophen-2-yl)acrylonitrile units at 3-, 5-, and 8-positions and the BODIPY core. **ST-3-BF₃** exhibited a characteristic fluorescence band originating from the BODIPY skeleton at around 730 nm. It was found that by addition of a trace amount of water to the acetonitrile solution of **ST-3-BF₃**, the photoabsorption band at around 415 nm and the fluorescence band at around 730 nm increased linearly as a function of the water content below only 0.2 wt%, which could be ascribed to the change in the ICT characteristics due to the dissociation of **ST-3-BF₃** into **ST-3** by water molecules. Thus, this work demonstrated that the 3,5,8-trithienyl-BODIPY-type pyridine–boron trifluoride complex can act as a highly-sensitive optical sensor for the detection of a trace amount of water in acetonitrile.

## Introduction

Optical methods utilizing colorimetric and fluorescent sensors for visualization as well as detection and quantification of water in samples and products, such as solutions, solids, and gases or water on substrate surfaces have been of considerable scientific and practical concern in recent years, because of not only fundamental studies in photochemistry, photophysics, and analytical chemistry, but also their potential applications to environmental and quality control monitoring systems and industry.[1–9] In fact, to date, some kinds of colorimetric and fluorescent sensors for water based on ICT (intramolecular charge transfer),[10,11] PET (photo-induced electron transfer),[12,13] or ESIP (excited state intramolecular proton transfer)[14] have been designed and developed. Among them, the ICT-type

sensor, which has a donor–π–acceptor (D–π–A) structure with photoabsorption and fluorescence properties originating from the ICT excitation from the electron-donating (D) moiety to the electron-accepting (A) moiety, allows colorimetric and ratio-metric fluorescence measurements, which are preferable because the ratio of photoabsorption or fluorescence intensities at two wavelengths is in fact independent of the total concentration of the sensor, photobleaching, fluctuations in light source intensity, sensitivity of the instrument, *etc.* Indeed, in ICT-type sensors based on a D–π–A structure for detecting cations, anions, and neutral organic species, the dipole moment and electronic structure changed due to the intermolecular interaction (electrostatic interaction) between the electron-donating or electron-accepting moiety of the sensors and the species, resulting in changes in photoabsorption, fluorescence (intensity and wavelength), and electrochemical properties (oxidation and reduction potentials) and enabling the detection (recognition) of the analytes. For this reason, we recently focused on D–π–A-type pyridine–boron trifluoride (BF₃) complexes as colorimetric and fluorescent sensors for water.[11] In our previous work, we have designed and actually developed

*Department of Applied Chemistry, Graduate School of Engineering, Hiroshima University, 1-4-1 Kagamiyama, Higashi-Hiroshima 739-8527, Japan. E-mail: kimato@hiroshima-u.ac.jp; yooyama@hiroshima-u.ac.jp; Fax: +81-82-424-5494*

† Electronic supplementary information (ESI) available. See DOI: 10.1039/d0ra06569b

a D–(π–A)₂-type pyridine–BF₃ complex **YNI-2-BF₃** composed of a carbazole skeleton as a donor moiety and two pyridine–BF₃ units as acceptor moieties (Fig. 1a).[11a] It was found that the blue-shift of the photoabsorption and the enhancement of the fluorescence intensity in the low-water-content region could be attributed to the change in the ICT characteristics due to the dissociation of **YNI-2-BF₃** into the D–(π–A)₂-type pyridine dye **YNI-2** by water molecules. Furthermore, a red-shift of fluorescence bands with a decrease in the fluorescence intensity in the high-water-content region was observed because of the formation of the hydrogen-bonded proton transfer (PTC) complex **YNI-2-H₂O** with water molecules. Moreover, 9-methyl pyrido [3,4-*b*]indole-BF₃ complex, **9-MP-BF₃**, was designed and developed as a colorimetric and ratiometric fluorescent sensor for the detection of water in the low-, moderate-, and high-water-content regions in solvents (Fig. 1b).[11b] It was found that in the low-water-content region, the blue-shifts of photoabsorption bands with an isosbestic point and fluorescence bands with an isoemissive point could be attributed to the dissociation of **9-MP-BF₃** into 9-methyl pyrido[3,4-*b*]indole (**9-MP**) by water molecules. In the moderate-water-content region, the photoabsorption and the fluorescence bands of **9-MP** gradually shifted to a longer wavelength region with the increase in the fluorescence intensity, which can be ascribed to the formation of the hydrogen-bonded complex (**9-MP-H₂O**) with water molecules. Furthermore, in the high-water-content region, two photoabsorption bands and one fluorescence band gradually reappeared in a longer wavelength region with simultaneous decreases in the photoabsorption and the fluorescence bands of **9-MP-H₂O**, which was attributed to the formation of the PTC complex (**9-MP-H⁺**) with water molecules. Consequently, our previous works proposed that the ICT-type pyridine–BF₃ complexes can act as colorimetric and fluorescent sensors for the detection of water in the low-, moderate-, and high-water-content regions in solvents.

In this work, in order to gain a further insight into the impacts of fluorophore and molecular structure on the optical sensing properties of ICT-type pyridine–BF₃ complexes for the detection of water, we designed and developed propeller-structured 3,5,8-trithienyl-BODIPY **ST-3** (ref. 15) and its pyridine–BF₃ complex **ST-3-BF₃**, which have three units of 2-(pyridin-4-yl)-3-(thiophen-2-yl)acrylonitrile as strong electron-withdrawing moiety at the 3-, 5-, and 8-positions on the BODIPY skeleton, leading to the bathochromic shift of the photoabsorption band due to the enhancement of the ICT characteristics (Fig. 1c). 4,4-Difluoro-4-bora-3*a*,4*a*-diaza-*s*-indacenes (boron dipyrromethene: BODIPY) dyes have created considerable interest as optical sensors and probes,[16] photosensitizers[17] for photodynamic therapy (PDT), and emitters[18] and dye-sensitizers[19] for optoelectronic devices such as organic light-emitting diodes (OLEDs) and dye-sensitized solar cells (DSSCs). It is expected that the addition of a trace amount of water to the solution of **ST-3-BF₃** causes the dissociation of **ST-3-BF₃** into **ST-3** by water molecules, resulting in the photoabsorption and fluorescence spectral changes. Herein we report the preparation, the characterization, and the optical sensing properties of the propeller-structured 3,5,8-trithienyl-BODIPY-
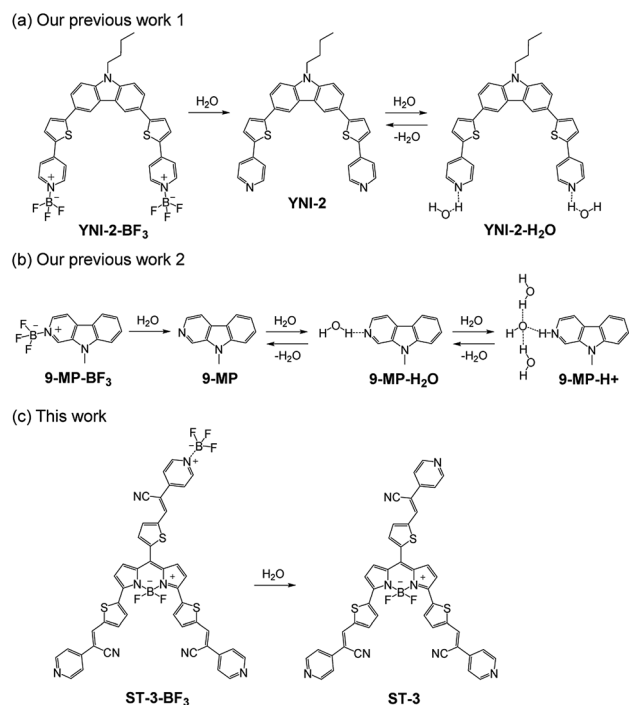


**Fig. 1** Proposed mechanisms of colorimetric and fluorescent sensors (a) **YNI-2-BF₃**, (b) **9-MP-BF₃**, and (c) propeller-structured BODIPY-type pyridine–boron trifluoride complex **ST-3-BF₃** for the detection of water in solvents.

type pyridine–BF₃ complex for the detection of a trace amount of water in acetonitrile based on FTIR, ¹H and ¹¹B NMR measurements, high-resolution mass spectrometry (HRMS) analysis, thermogravimetry-differential thermal analysis (TG-DTA), photoabsorption and fluorescence spectral measurements of **ST-3-BF₃** in acetonitrile containing various concentrations of water, and density functional theory (DFT) calculations.

## Results and discussion

### Characterization of ST-3-BF₃

The propeller-structured 3,5,8-trithienyl-BODIPY-type pyridine–BF₃ complex **ST-3-BF₃** studied in this work was prepared by treating **ST-3** (ref. 15) with boron trifluoride diethyl etherate
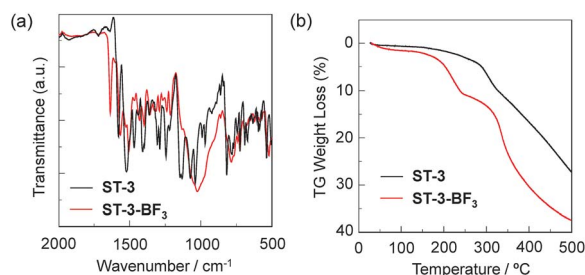


**Fig. 2** (a) FTIR spectra of **ST-3** and **ST-3-BF₃**. (b) TG curves for **ST-3** and **ST-3-BF₃** at a heating rate of 10 °C min⁻¹.
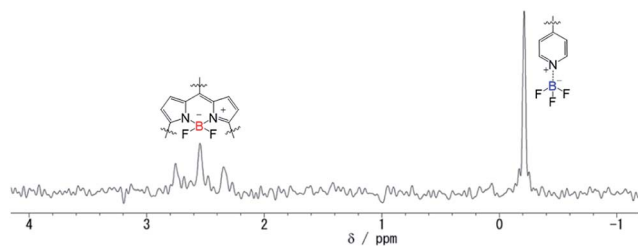
**Fig. 3** $^{11}$B NMR spectrum of **ST-3-BF$_3$** in acetonitrile-$d_3$.



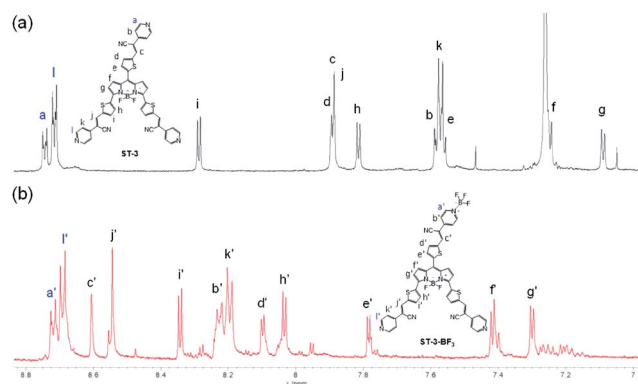**Fig. 4** $^1$H NMR spectra of (a) **ST-3** in CDCl$_3$ and (b) **ST-3-BF$_3$** in acetonitrile-$d_3$.

(BF$_3$–OEt$_2$) and fully characterized by FTIR, $^1$H and $^{11}$B NMR measurements, HRMS, and TG-DTA, although we could not obtain the $^{13}$C NMR spectrum that is clear enough to be assigned, due to the low solubility of **ST-3-BF$_3$** into solvent (Fig. 2–4). In the FTIR spectra, the B–F and B–N stretching bands originating from the BODIPY core were observed at 1082 and 1522 cm$^{-1}$ for **ST-3** and 1047 and 1504 cm$^{-1}$ for **ST-3-BF$_3$**, respectively (Fig. 2a). In addition, for **ST-3-BF$_3$**, the characteristic C=N stretching band of the pyridyl group coordinated to BF$_3$, the B–N stretching band of the pyridine–BF$_3$ complex, and the B–F stretching band of BF$_3$ were clearly observed at 1636, 1429, and 1024 cm$^{-1}$, respectively. The TG-DTA of **ST-3-BF$_3$** indicated the decreased weight loss by 7.78% in comparison with that of **ST-3** at around 275 °C, which is in good agreement with the calculated weight loss of 7.61% for the release of a BF$_3$ unit from **ST-3-BF$_3$** (Fig. 2b). Moreover, the $^{11}$B NMR spectrum of **ST-3-BF$_3$** in acetonitrile-$d_3$ showed a singlet at −0.21 ppm, which can be assigned to BF$_3$ coordinated to the pyridyl group, and a characteristic triplet with coupling constant ($J_{B-F}$) of 33 Hz at around 2–3 ppm, which indicates the presence of the BF$_2$ group in BODIPY (Fig. 3). Based on this result, the ratio of the peak integrals of BF$_3$ and BF$_2$ was 1 : 1. Obviously, the FTIR, TG-DTA, and $^{11}$B NMR results demonstrated the presence of one BF$_3$ unit coordinated to the pyridyl group in **ST-3-BF$_3$**, although HRMS (ESI) of **ST-3-BF$_3$** showed the base peak corresponding to the molecular ion for $m/z$ of [ST-3 + 2H]$^{2+}$ (calcd for C$_{45}$H$_{27}$N$_8$BF$_2$S$_3$, 412.07855; found 412.07918) due to the measurement condition.

For the $^1$H NMR spectrum of the propeller-structured 3,5,8-trithienyl-BODIPY-type pyridine–BF$_3$ complex, if it is assumed that BF$_3$ coordinates to a pyridyl group at the end of the 3- or 5-position on the BODIPY core, the $^1$H NMR spectrum of **ST-3-BF$_3$** is expected to be more complex than that of **ST-3**. For example, the 1-position protons on the pyridyl groups at the end of the 3-, 5-, and 8-positions on the BODIPY core will appear as three different signals. On the other hand, if it is assumed that BF$_3$ coordinates to the pyridyl group at the end of the 8-position on the BODIPY core, the signal pattern in the $^1$H NMR spectrum of **ST-3-BF$_3$** is expected to be similar to that of **ST-3**. In fact, the $^1$H NMR spectrum of **ST-3-BF$_3$** demonstrated that the chemical shifts and signal pattern of the 1-position protons ($H_{a'}$ and $H_{l'}$) on the pyridyl groups of **ST-3-BF$_3$** show little change from those ($H_a$ and $H_l$) of **ST-3**, indicating the formation of the pyridine–BF$_3$ complex coordinated to the pyridyl group at the end of the 8-position on the BODIPY core (Fig. 4), although the comparison of the $^1$H NMR spectra between **ST-3** and **ST-3-BF$_3$** might be difficult because different deuterated solvents were used for **ST-3** (in CDCl$_3$) and **ST-3-BF$_3$** (in acetonitrile-$d_3$).

The photoabsorption spectra of **ST-3** and **ST-3-BF$_3$** in acetonitrile revealed that the two dyes show a strong and broad photoabsorption band in the range of 600 to 800 nm, which is assigned to the S$_0$ → S$_1$ transition of the BODIPY skeleton with the expanded π-conjugated system over the 2-(pyridin-4-yl)-3-(thiophen-2-yl)acrylonitrile units at the 3-, 5-, and 8-positions onto the BODIPY core (Fig. 5a). In addition, a photoabsorption band was also observed in the range of 300 to 550 nm, which can be assigned to the ICT band between the 2-(pyridin-4-yl)-3-(thiophen-2-yl)acrylonitrile units at 3-, 5-, and 8-positions and the BODIPY core.[15,20] It is worth noting here that for **ST-3**, the peak absorbance of the former photoabsorption band at 695 nm is comparable with that of the latter ICT band at 415 nm, while for **ST-3-BF$_3$**, the peak absorbance of the former band at 695 nm is lower than that of the latter band at 415 nm, which is attributed to the enhanced ICT characteristics. Moreover, for **ST-3**, the peak absorbance at 415 nm is higher than that at 450 nm, whereas for **ST-3-BF$_3$**, the peak absorbance at 415 nm is lower than that at 465 nm. The corresponding fluorescence spectra of the two dyes show a characteristic fluorescence band at around 730 nm originating from the BODIPY skeleton, and the fluorescence band of **ST-3-BF$_3$** is broader than that of **ST-3** (Fig. 5b). Consequently, the characterization of the propeller-structured 3,5,8-trithienyl-
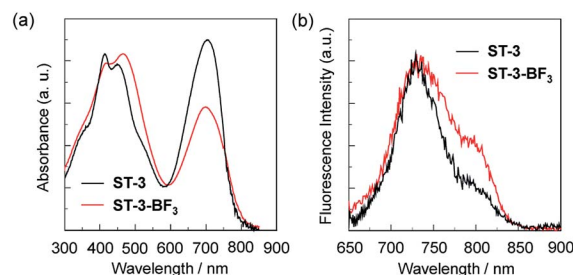


**Fig. 5** (a) Photoabsorption and (b) fluorescence ($\lambda_{ex}$ = 640 nm) spectra of **ST-3** and **ST-3-BF$_3$** in acetonitrile.
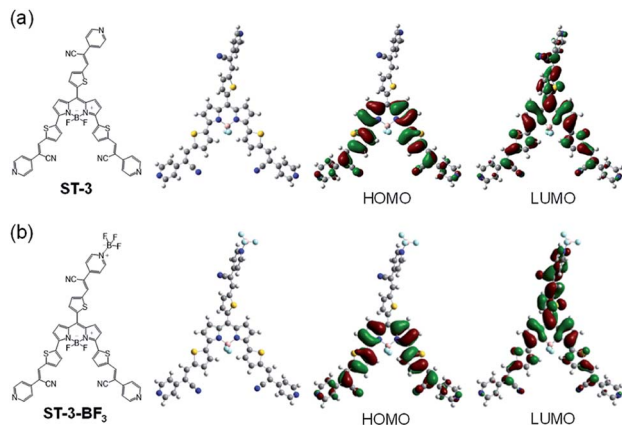
**Fig. 6** Optimized geometries, HOMOs, and LUMOs of (a) **ST-3** and (b) **ST-3-BF₃** derived from DFT calculations at the B3LYP/6–31G(d,p) level.



**Fig. 7** (a) Photoabsorption and (b) fluorescence spectra ($\lambda_{ex}$ = 640 nm) of **ST-3-BF₃** ($c = 2.5 \times 10^{-6}$ M) in acetonitrile containing water (0.0046–0.98 wt%).



**Fig. 8** (a) Absorbance at 415 and 695 nm, and (b) fluorescence peak intensity at around 730 nm ($\lambda_{ex}$ = 640 nm) of **ST-3-BF₃** as a function of water content below 1.0 wt% in acetonitrile.

BODIPY-type pyridine–BF₃ complex is successfully determined by the photoabsorption and fluorescence spectral measurements as well as FTIR, $^{1}$H and $^{11}$B NMR, HRMS, and TG-DTA. In order to examine the electronic structures of the propeller-structured 3,5,8-trithienyl-BODIPY dyes, the molecular structures and molecular orbitals of **ST-3** and **ST-3-BF₃** were calculated using DFT at the B3LYP/6-31G(d,p) level (Fig. 6). For the two dyes, the HOMOs are mostly localized on the BODIPY core and the two thienyl groups at the 3- and 5-positions. On the other hand, the LUMO of **ST-3** is mostly localized on the BODIPY core and the three thienyl groups at the 3-, 5-, and 8-positions, but that of **ST-3-BF₃** is mostly localized not only on the BODIPY core and the two thienyl groups at the 3- and 5-positions but also over the 2-(pyridin-4-yl)-3-(thiophen-2-yl)acrylonitrile unit at the 8-position. Thus, the DFT calculations suggest that the dissociation of **ST-3-BF₃** into **ST-3** by water molecules results in the photoabsorption and fluorescence spectral changes based on their ICT characteristics due to the perturbation in the LUMO over the 2-(pyridin-4-yl)-3-(thiophen-2-yl)acrylonitrile unit of **ST-3-BF₃**.

### Optical sensing ability of ST-3-BF₃ for water in acetonitrile

In order to investigate the optical sensing ability of **ST-3-BF₃** for water in acetonitrile, the photoabsorption and fluorescence spectra of **ST-3-BF₃** were measured in acetonitrile that contained various concentrations of water (Fig. 7). With the increase in the water content in acetonitrile solution, a red-shift of the photoabsorption band at 465 nm with a decrease in the absorbance and simultaneous increases in the absorbance of the two photoabsorption bands at around 415 and 695 nm were observed, which could be ascribed to the dissociation of **ST-3-BF₃** into **ST-3** by water molecules (Fig. 7a). On the other hand, the corresponding fluorescence spectra of **ST-3-BF₃** underwent an increase in the intensity of the fluorescence band at around 730 nm (Fig. 7b). To estimate the sensitivity and accuracy characteristics of **ST-3-BF₃** for the detection of water in acetonitrile, the changes in the absorbance and fluorescence intensity were plotted against the water fraction in acetonitrile (Fig. 8). The plots of absorbance in the water content region
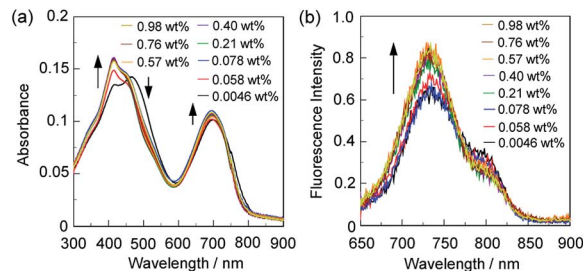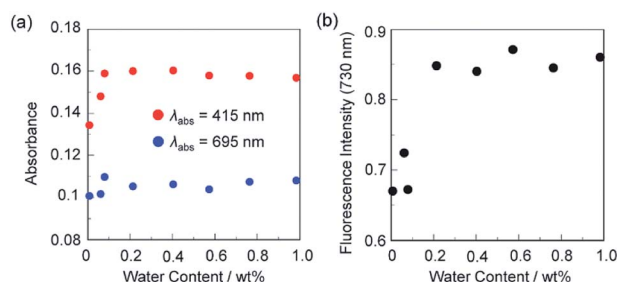
below 1.0 wt% demonstrated that the absorbance at around 415 nm increased linearly as a function of the water content, but the absorbance at around 695 nm slightly increased as a function of the water content (Fig. 8a). Moreover, the plot of fluorescence intensity at around 730 nm in the water content region below 1.0 wt% demonstrates that the fluorescence peak intensity increases almost linearly as a function of the water content (Fig. 8b). The increases in the absorbance and fluorescence intensity leveled off in the water content region above 0.2 wt%. Thus, it was found that the addition of a trace amount of water to the acetonitrile solution of **ST-3-BF₃** causes the change in the ICT characteristics due to the dissociation of **ST-3-BF₃** into **ST-3** by water molecules, and as the result, the photoabsorption band at around 415 nm and the fluorescence band at around 730 nm increase linearly as a function of the water content below only 0.2 wt%. Consequently, this work demonstrated that the 3,5,8-trithienyl-BODIPY-type pyridine–BF₃ complex can act as a high-sensitive optical sensor for the detection of a trace amount of water in acetonitrile.

## Conclusions

We have designed and developed the propeller-structured 3,5,8-trithienyl-BODIPY-type pyridine–boron trifluoride complex, **ST-3-BF₃**, which has three units of 2-(pyridin-4-yl)-3-(thiophen-2-yl)acrylonitrile at the 3-, 5-, and 8-positions on the BODIPY skeleton, as an intramolecular charge transfer (ICT)-type optical sensor for the detection of a trace amount of water in acetonitrile. It was found that the addition of a trace amount of water to

the acetonitrile solution of **ST-3-BF₃** causes the photoabsorption and fluorescence spectral changes based on the ICT characteristics due to the dissociation of **ST-3-BF₃** into **ST-3** by water molecules. Indeed, the absorbance and fluorescence intensity increased linearly as a function of the water content below only 0.2 wt%. Based on the optical sensing mechanism of **ST-3-BF₃**, we demonstrated that the 3,5,8-trithienyl-BODIPY-type pyridine–boron trifluoride complex can act as a high-sensitive optical sensor for the detection of a trace amount of water in acetonitrile. Thus, our continuous works regarding optical sensors for water confirm that the ICT-type pyridine–boron trifluoride complex is one of the most promising colorimetric and fluorescent sensors for the detection of water in the low-, moderate-, and high-water-content regions in solvents. Moreover, NIR dyes such as ICT-type pyridine–boron trifluoride complex which make it possible to control the intensity of NIR luminescence by the presence or absence of water, may be applicable to the wavelength conversion dye-doped films for controlling the plant growth (photomorphogenesis).

## Experimental

### General

IR spectra were recorded on a SHIMADZU IRTracer-100 using ATR method. $^1$H NMR and $^{11}$B NMR spectra were recorded on a Varian-500 (500 MHz) FT NMR spectrometer. High-resolution mass spectral data by ESI were acquired on a Thermo Fisher Scientific LTQ Orbitrap XL. Photoabsorption spectra were observed with a SHIMADZU UV-3150 spectrophotometer. Fluorescence spectra were measured with a Hitachi F-4500 spectrophotometer. Super dehydrated acetonitrile was used for all the experiments. The addition of water to acetonitrile solutions containing **ST-3-BF₃** was made by weight percent (wt%). The determination of water in acetonitrile was done with an MKC-610 and MKA-610 Karl Fischer moisture titrator (Kyoto Electronics manufacturing Co., Ltd.) based on Karl Fischer coulometric titration.

### Synthesis

**(2Z,2′Z,2″Z)-3,3′,3″-((5,5-difluoro-5H-4l4,5l4-dipyrrolo[1,2-c:2′,1′-f][1,3,2]diazaborinine-3,7,10-triyl)tris(thiophene-5,2-diyl))tris(2-(pyridin-4-yl)acrylonitrile)-boron trifluoride complex (ST-3-BF₃).** To a solution of **ST-3** (ref. 15) (5.0 mg, 6.1 μmol) in acetonitrile (5.0 mL) under a nitrogen atmosphere was added dropwise 47% BF₃–OEt₂ (4.6 μL, 37 μmol) diluted with acetonitrile (1.0 mL) for 10 min, and then, the solution was stirred for 3 h at room temperature. Next, to toluene was added dropwise the reaction mixture, and then, the resulting precipitate was filtered to give **ST-3-BF₃** (4.0 mg, 74% yield) as a black solid; FT-IR (ATR): $\tilde{v}$ = 1636 (C=N str. for pyridyl group coordinated to BF₃), 1504 (B–N str. for BODIPY core), 1429 (B–N str. for pyridine–BF₃ complex), 1047 (B–F str. for BF₂ in BODIPY core), 1024 (B–F str. for BF₃) cm$^{-1}$; $^1$H NMR (500 MHz, acetonitrile-$d_3$): δ = 7.30 (d, $J$ = 4.5 Hz, 2H), 7.42 (d, $J$ = 4.7 Hz, 2H), 7.78 (d, $J$ = 4.0 Hz, 1H), 8.03 (d, $J$ = 4.3 Hz, 2H), 8.10 (d, $J$ = 3.8 Hz, 1H), 8.20 (d, $J$ = 7.0 Hz, 4H), 8.23 (d, $J$ = 7.5 Hz, 2H), 8.34 (d, $J$ = 4.3 Hz, 2H), 8.54 (s, 2H), 8.61 (s, 1H), 8.69 (d, $J$ = 7.0 Hz, 4H), 8.72 (d, $J$ = 7.1 Hz, 2H) ppm; $^{11}$B NMR (160 MHz, acetonitrile-$d_3$) δ = −0.21 (s), 2.55 (t, $J_{B-F}$ = 33 Hz) ppm; HRMS (ESI): $m/z$ (%): [M + 2H]$^{2+}$ calcd for C₄₅H₂₇N₈BF₂S₃, 412.07855; found 412.07918.

## Conflicts of interest

There are no conflicts to declare.

## Acknowledgements

## Notes and references

1 H. S. Jung, P. Verwilst, W. Y. Kim and J. S. Kim, Fluorescent and colorimetric sensors for the detection of humidity or water content, *Chem. Soc. Rev.*, 2016, **45**, 1242–1256.

2 W.-E. Lee, Y.-J. Jin, L.-S. Park and G. Kwak, Fluorescent Actuator Based on Microporous Conjugated Polymer with Intramolecular Stack Structure, *Adv. Mater.*, 2012, **24**, 5604–5609.

3 A. Douvali, A. C. Tsipis, S. V. Eliseeva, S. Petoud, G. S. Papaefstathiou, C. D. Malliakas, I. Papadas, G. S. Armatas, I. Margiolaki, M. G. Kanatzidis, T. Lazarides and M. J. Manos, Turn-On Luminescence Sensing and Real-Time Detection of Traces of Water in Organic Solvents by a Flexible Metal–Organic Framework, *Angew. Chem., Int. Ed.*, 2015, **54**, 1651–1656.

4 J. Lee, M. Pyo, S. Lee, J. Kim, M. Ra, W.-Y. Kim, B. J. Park, C. W. Lee and J.-M. Kim, Hydrochromic conjugated polymers for human sweat pore mapping, *Nat. Commun.*, 2014, **5**, 3736.

5 (*a*) Q. Deng, Y. Li, J. Wu, Y. Liu, G. Fang, S. Wang and Y. Zhang, Highly sensitive fluorescent sensing for water based on poly(m-aminobenzoic acid), *Chem. Commun.*, 2012, **48**, 3009–3011; (*b*) L. Ding, Z. Zhang, X. Li and J. Su, Highly sensitive determination of low-level water content in organic solvents using novel solvatochromic dyes based on thioxanthone, *Chem. Commun.*, 2013, **49**, 7319–7321; (*c*) M. Tanioka, S. Kamino, A. Muranaka, Y. Shirasaki, Y. Ooyama, M. Ueda, M. Uchiyama, S. Enomoto and D. Sawada, Water-tunable solvatochromic and nanoaggregate fluorescence: dual colour visualisation and quantification of trace water in tetrahydrofuran, *Phys. Chem. Chem. Phys.*, 2017, **19**, 1209–1216; (*d*) D. Wang, H. Zhao, H. Li, S. Sun and Y. Xu, A fluorescent "glue" of water triggered by hydrogen-bonding cross-linking, *J. Mater. Chem. C*, 2016, **4**, 11050–11054; (*e*) S. Guo, Y. Ma, S. Li, Q. Yu, A. Xu, J. Han, L. Wei, Q. Zhao and W. Huang, A phosphorescent Ir(III) complex with formamide for the luminescence determination of low-level water content in organic solvents, *J. Mater. Chem. C*, 2016, **4**, 6110–6116; (*f*) Y. Dong, J. Cai, Q. Fang, X. You and Y. Chi, Dual-Emission

of Lanthanide Metal–Organic Frameworks Encapsulating Carbon-Based Dots for Ratiometric Detection of Water in Organic Solvents, *Anal. Chem.*, 2016, **88**, 1748–1752; (*g*) Y. Huang, W. Liu, H. Feng, Y. Ye, C. Tang, H. Ao, M. Zhao, G. Chen, J. Chen and Z. Qian, Luminescent Nanoswitch Based on Organic-Phase Copper Nanoclusters for Sensitive Detection of Trace Amount of Water in Organic Solvents, *Anal. Chem.*, 2016, **88**, 7429–7434; (*h*) P. Kumar, R. Kaushik, A. Ghosh and A. Jose, Detection of Moisture by Fluorescent OFF-ON Sensor in Organic Solvents and Raw Food Products, *Anal. Chem.*, 2016, **88**, 11314–11318; (*i*) Y. Zhang, C. Liarg and S. Jiang, A solvatochromic cyanostilbene derivative as an intensity and wavelength-based fluorescent sensor for water in organic solvents, *New J. Chem.*, 2017, **41**, 8644–8649.

6 (*a*) A. Wang, R. Fan, Y. Dong, Y. Song, Y. Zhou, J. Zheng, X. Du, K. Xing and Y. Yang, Detection and Monitoring of Amyloid Fibrillation Using a Fluorescence "Switch-On" Probe, *ACS Appl. Mater. Interfaces*, 2017, **9**, 15744–15757; (*b*) A. Wang, R. Fan, Y. Dong, W. Chen, Y. Song, P. Wang, S. Hao, Z. Liu and Y. Yang, (*E*)-4-Methyl-*N*-((quinolin-2-yl) ethylidene)aniline as ligand for IIB supramolecular complexes: synthesis, structure, aggregation-induced emission enhancement and application in PMMA-doped hybrid material, *Dalton Trans.*, 2017, **46**, 71–85; (*c*) A. Wang, R. Fan, P. Wang, R. Fang, S. Hao, X. Zhou, X. Zheng and Y. Yang, Research on the Mechanism of Aggregation-Induced Emission through Supramolecular Metal-Organic Frameworks with Mechanoluminescent Properties and Application in Press-Jet Printing, *Inorg. Chem.*, 2017, **56**, 12881–12892; (*d*) H.-L. Qian, C. Dai, C.-X. Yang and X.-P. Yan, High-Crystallinity Covalent Organic Framework with Dual Fluorescence Emissions and Its Ratiometric Sensing Application, *ACS Appl. Mater. Interfaces*, 2017, **9**, 24999–25005.

7 (*a*) P. Kumar, R. Sakla, A. Ghosh and D. A. Jose, Reversible Colorimetric Sensor for Moisture Detection in Organic Solvents and Application in Inkless Writing, *ACS Appl. Mater. Interfaces*, 2017, **9**, 25600–25605; (*b*) S. Song, Y. Zhang, Y. Yang, C. Wang, Y. Zhou, C. Zhang, Y. Zhao, M. Yang and Q. Lin, Ratiometric fluorescence detection of trace water in organic solvents based on aggregation-induced emission enhanced Cu nanoclusters, *Analyst*, 2018, **143**, 3068–3074; (*c*) E. Poonia, P. K. Mishra, V. Kiran, J. Sangwan, R. Kumar, P. K. Rai and V. K. Tomer, Aero-gel assisted synthesis of anatase TiO$_2$ nanoparticles for humidity sensing application, *Dalton Trans.*, 2018, **47**, 6293–6298; (*d*) H. Yan, S. Guo, F. Wu, P. Yu, H. Liu, Y. Li and L. Mao, Carbon Atom Hybridization Matters: Ultrafast Humidity Response of Graphdiyne Oxides, *Angew. Chem., Int. Ed.*, 2018, **57**, 3922–3926.

8 (*a*) Y. Zhou, G. Baryshnikov, X. Li, M. Zhu, H. Ågren and L. Zhu, Anti-Kasha's Rule Emissive Switching Induced by Intermolecular H-Bonding, *Chem. Mater.*, 2018, **30**, 8008–8016; (*b*) J. Wei, H. Li, Y. Yuan, C. Sun, D. Hao, G. Zheng and R. Wang, A sensitive fluorescent sensor for the detection of trace water in organic solvents based on

carbon quantum dots with yellow fluorescence, *RSC Adv.*, 2018, **8**, 37028–37034; (*c*) S. Song, Y. Zhang, Y. Yang, C. Wang, Y. Zhou, C. Zhang, Y. Zhao, M. Yang and Q. Lin, Ratiometric fluorescence detection of trace water in organic solvents based on aggregation-induced emission enhanced Cu nanoclusters, *Analyst*, 2018, **143**, 3068–3074.

9 (*a*) T. Maeda and F. Würthner, Halochromic and hydrochromic squaric acid functionalized perylene bisimide, *Chem. Commun.*, 2015, **51**, 7661–7664; (*b*) S. Pawar, U. K. Togiti, A. Bhattacharya and A. Nag, Functionalized Chitosan–Carbon Dots: A Fluorescent Probe for Detecting Trace Amount of Water in Organic Solvents, *ACS Omega*, 2019, **4**, 11301–11311; (*c*) F. Wu, L. Wang, H. Tang and D. Cao, Excited State Intramolecular Proton Transfer Plus Aggregation-Induced Emission-Based Diketopyrrolopyrrole Luminogen: Photophysical Properties and Simultaneously Discriminative Detection of Trace Water in Three Organic Solvents, *Anal. Chem.*, 2019, **91**, 5261–5269; (*d*) W. Cheng, Y. Xie, Z. Yang, Y. Sun, M.-Z. Zhang, Y. Ding and W. Zhang, General Strategy for in Situ Generation of a Coumarin-Cu$^{2+}$ Complex for Fluorescent Water Sensing, *Anal. Chem.*, 2019, **91**, 5817–5823.

10 (*a*) D. Citterio, K. Minamihashi, Y. Kuniyoshi, H. Hisamoto, S. Sasaki and K. Suzuki, Optical Determination of Low-Level Water Concentrations in Organic Solvents Using Fluorescent Acridinyl Dyes and Dye-Immobilized Polymer Membranes, *Anal. Chem.*, 2001, **73**, 5339–5345; (*b*) C.-G. Niu, A.-L. Guan, G.-M. Zeng, Y.-G. Liu and Z.-W. Li, Fluorescence water sensor based on covalent immobilization of chalcone derivative, *Anal. Chim. Acta*, 2006, **577**, 264–270; (*c*) C.-G. Niu, P.-Z. Qin, G.-M. Zeng, X.-Q. Gui and A.-L. Guan, Fluorescence sensor for water in organic solvents prepared from covalent immobilization of 4-morpholinyl-1, 8-naphthalimide, *Anal. Bioanal. Chem.*, 2007, **387**, 1067–1074; (*d*) Z.-Z. Li, C.-G. Niu, G.-M. Zeng and P.-Z. Qin, Fluorescence Sensor for Water Content in Organic Solvents Based on Covalent Immobilization of Benzothioxanthene, *Chem. Lett.*, 2009, **38**, 698–699; (*e*) Z. Li, Q. Yang, R. Chang, G. Ma, M. Chen and W. Zhang, N-Heteroaryl-1,8-naphthalimide fluorescent sensor for water: Molecular design, synthesis and properties, *Dyes Pigm.*, 2011, **88**, 307–314; (*f*) Y. Zhang, D. Li, Y. Li and J. Yu, Solvatochromic AIE luminogens as supersensitive water detectors in organic solvents and highly efficient cyanide chemosensors in water, *Chem. Sci.*, 2014, **5**, 2710–2716; (*g*) W. Chen, Z. Zhang, X. Li, H. Ågren and J. Su, Highly sensitive detection of low-level water content in organic solvents and cyanide in aqueous media using novel solvatochromic AIEE fluorophores, *RSC Adv.*, 2015, **5**, 12191–12201.

11 (*a*) S. Tsumura, T. Enoki and Y. Ooyama, A colorimetric and fluorescent sensor for water in acetonitrile based on intramolecular charge transfer: D–(π–A)$_2$-type pyridine–boron trifluoride complex, *Chem. Commun.*, 2018, **54**, 10144–10147; (*b*) T. Enoki and Y. Ooyama, Colorimetric and ratiometric fluorescence sensing of water based on 9-methyl pyrido[3,4-*b*]indole-boron trifluoride complex,

*Dalton Trans.*, 2019, **48**, 2086–2092; (*c*) K. Imato, T. Enoki and Y. Ooyama, Development of an intramolecular charge transfer-type colorimetric and fluorescence sensor for water by fusion with a juloidine structure and complexation with boron trifluoride, *RSC Adv.*, 2019, **9**, 31466–31473.

12 (*a*) Y. Ooyama, M. Sumomogi, T. Nagano, K. Kushimoto, K. Komaguchi, I. Imae and Y. Harima, Detection of water in organic solvents by photo-induced electron transfer method, *Org. Biomol. Chem.*, 2011, **9**, 1314–1316; (*b*) Y. Ooyama, A. Matsugasako, T. Nagano, K. Oka, K. Kushimoto, K. Komaguchi, I. Imae and Y. Harima, Fluorescence PET (photo-induced electron transfer) sensor for water based on anthracene-amino acid, *J. Photochem. Photobiol., A*, 2011, **222**, 52–55.

13 (*a*) Y. Ooyama, A. Matsugasako, K. Oka, T. Nagano, M. Sumomogi, K. Komaguchi, I. Imae and Y. Harima, Fluorescence PET (photo-induced electron transfer) sensors for water based on anthracene–boronic acid ester, *Chem. Commun.*, 2011, **47**, 4448–4450; (*b*) Y. Ooyama, A. Matsugasako, Y. Hagiwara, J. Ohshita and Y. Harima, Highly sensitive fluorescence PET (photo-induced electron transfer) sensor for water based on anthracene–bisboronic acid ester, *RSC Adv.*, 2012, **2**, 7666–7668; (*c*) Y. Ooyama, K. Uenaka, A. Matsugasako, Y. Harima and J. Ohshita, Molecular design and synthesis of fluorescence PET (photo-induced electron transfer) sensors for detection of water in organic solvents, *RSC Adv.*, 2013, **3**, 23255–23263; (*d*) Y. Ooyama, K. Furue, K. Uenaka and J. Ohshita, Development of highly-sensitive fluorescence PET (photo-induced electron transfer) sensor for water: anthracene–boronic acid ester, *RSC Adv.*, 2014, **4**, 25330–25333; (*e*) Y. Ooyama, S. Aoyama, K. Furue, K. Uenaka and J. Ohshita, Fluorescence sensor for water based on PET (photo-induced electron transfer): Anthracene-bis(aminomethyl) phenylboronic acid ester, *Dyes Pigm.*, 2015, **123**, 248–253; (*f*) Y. Ooyama, M. Hato, T. Enoki, S. Aoyama, K. Furue, N. Tsunoji and J. Ohshita, A BODIPY sensor for water based on a photo-induced electron transfer method with fluorescence enhancement and attenuation systems, *New J. Chem.*, 2016, **40**, 7278–7281; (*g*) Y. Ooyama, R. Nomura, T. Enoki, R. Sagisaka, N. Tsunoji and J. Ohshita, Development of a Dual-Fluorescence Emission Sensor Based on Photo-Induced Electron Transfer and Aggregation-Induced Emission Enhancement for Detection of Water, *ChemistrySelect*, 2017, **2**, 7765–7770; (*h*) Y. Ooyama, R. Sagisaka, T. Enoki, N. Tsunoji and J. Ohshita, Tetraphenylethene – and diphenyldibenzofulvene–anthracene-based fluorescence sensors possessing photo-induced electron transfer and aggregation-induced emission enhancement characteristics for detection of water, *New J. Chem.*, 2018, **42**, 13339–13350.

14 (*a*) W. Liu, Y. Wang, W. Jin, G. Shen and R. Yu, Solvatochromogenic flavone dyes for the detection of water in acetone, *Anal. Chim. Acta*, 1999, **383**, 299–307; (*b*) H. Mishra, V. Misra, M. S. Mehata, T. C. Pant and H. B. Tripathi, Fluorescence Studies of Salicylic Acid Doped Poly(vinyl alcohol) Film as a Water/Humidity Sensor, *J. Phys. Chem. A*, 2004, **108**, 2346–2352; (*c*) A. C. Kumar and A. K. Mishra, 1-Naphthol as an excited state proton transfer fluorescent probe for sensing bound-water hydration of polyvinyl alcohol, *Talanta*, 2007, **71**, 2003–2006.

15 S. Tsumura, K. Ohira, K. Hashimoto, K. Imato and Y. Ooyama, Synthesis, optical and electrochemical properties of propeller-type 3,5,8-trithienyl-BODIPY dyes, *Mater. Chem. Front.*, 2020, **4**, 2762–2771.

16 (*a*) Y. Zhao, Y. Zhang, X. Lv, Y. Liu, M. Chen, P. Wang, J. Liu and W. Guo, Through-bond energy transfer cassettes based on coumarin–Bodipy/distyryl Bodipy dyads with efficient energy efficiencies and large pseudo-Stokes' shifts, *J. Mater. Chem.*, 2011, **21**, 13168–13171; (*b*) M. Baruah, W. Qin, N. Basarić, W. M. Dw Borggraev and N. Boens, BODIPY-Based Hydroxyaryl Derivatives as Fluorescent pH Probes, *J. Org. Chem.*, 2005, **70**, 4152–4157; (*c*) X. Kong, L. Di, Y. Fan, Z. Zhou, X. Feng, L. Gai, J. Tian and H. Lu, Lysosome-targeting turn-on red/NIR BODIPY probes for imaging hypoxic cells, *Chem. Commun.*, 2019, **55**, 11567–11570; (*d*) F.-K. Tang, J. Zhu, F. K.-W. Kong, M. Ng, Q. Bian, V. W.-W. Yam, A. K.-W. Tse, Y.-C. Tse and K. C.-F. Leung, A BODIPY-based fluorescent sensor for the detection of Pt²⁺ and Pt drugs, *Chem. Commun.*, 2020, **56**, 2695–2698; (*e*) W. Chi, J. Chen, W. Liu, C. Wang, Q. Qi, Q. Qiao, T. M. Tan, K. Xiong, X. Liu, K. Kang, Y.-T. Chang, Z. Xu and X. Liu, A General Descriptor ΔE Enables the Quantitative Development of Luminescent Materials Based on Photoinduced Electron Transfer, *J. Am. Chem. Soc.*, 2020, **142**, 6777–6785; (*f*) D. Kand, P. Liu, M. X. Navarro, L. J. Fischer, L. Rousso-Noori, D. Friedmann-Morvinski, A. H. Winter, E. W. Miller and R. Weinstain, Water-Soluble BODIPY Photocages with Tunable Cellular Localization, *J. Am. Chem. Soc.*, 2020, **142**, 4970–4974.

17 (*a*) S. G. Awuah and Y. You, Boron dipyrromethene (BODIPY)-based photosensitizers for photodynamic therapy, *RSC Adv.*, 2012, **2**, 11169–11183; (*b*) A. Kamkaew, S. H. Lim, H. B. Lee, L. V. Kiew, L. Y. Chung and K. Burgess, BODIPY dyes in photodynamic therapy, *Chem. Soc. Rev.*, 2013, **42**, 77–88; (*c*) Y. Cakmak, S. Kolemen, S. Duman, Y. Dede, Y. Dolen, B. Kilic, Z. Kostereli, L. T. Yildirim, A. L. Dogan, D. Guc and E. U. Akkaya, Designing Excited States: Theory-Guided Access to Efficient Photosensitizers for Photodynamic Action, *Angew. Chem., Int. Ed.*, 2011, **50**, 11937–11941; (*d*) Y. Liu, C. Xu, L. Teng, H.-W. Liu, T.-B. Ren, S. Xu, X. Lou, H. Guo, L. Yuan and X.-B. Zhang, pH stimulus-disaggregated BODIPY: an activated photodynamic/photothermal sensitizer applicable to tumor ablation, *Chem. Commun.*, 2020, **56**, 1956–1959; (*e*) Y. Su, S. Lu, P. Gao, M. Zheng and Z. Xie, BODIPY@carbon dot nanocomposites for enhanced photodynamic activity, *Mater. Chem. Front.*, 2019, **3**, 1747–1753; (*f*) J. Jiménez, R. Prieto-Montero, B. L. Maroto, F. Moreno, M. J. Ortiz, A. Oliden-Sánchez, I. López-Arbeloa, V. Martínez-Martínez and S. de la Moya, Manipulating Charge-Transfer States in BODIPYs: A Model Strategy to

Rapidly Develop Photodynamic Theragnostic Agents, *Chem.– Eur. J.*, 2020, **26**, 601–605.

18 (*a*) A. Zampetti, A. Minotto, B. M. Squeo, V. G. Gregoriou, S. Allard, U. Scherf, C. L. Chochos and F. Cacialli, Highly Efficient Solid-State Near-infrared Organic Light-Emitting Diodes incorporating A-D-A Dyes based on α,β-unsubstituted "BODIPY" Moieties, *Sci. Rep.*, 2017, **7**, 1611; (*b*) A. Zampetti, A. Minotto and F. Cacialli, Near-Infrared (NIR) Organic Light-Emitting Diodes (OLEDs): Challenges and Opportunities, *Adv. Funct. Mater.*, 2019, **29**, 1807623.

19 (*a*) D. Kumaresan, R. P. Thummel, T. Bura, G. Ulrich and R. Ziessel, Color Tuning in New Metal-Free Organic Sensitizers (Bodipys) for Dye-Sensitized Solar Cells, *Chem.– Eur. J.*, 2009, **15**, 6335–6339; (*b*) S. Erten-Ela, M. D. Yilmaz, B. Icli, Y. Dede, S. Icli and E. U. Akkaya, A Panchromatic Boradiazaindacene (BODIPY) Sensitizer for Dye-Sensitized Solar Cells, *Org. Lett.*, 2008, **10**, 3299–3302; (*c*) S. Kolemen, O. A. Bozdemir, Y. Cakmak, G. Barin, S. Erten-Ela, M. Marszalek, J.-H. Yum, S. M. Zakeeruddin, M. K. Nazeeruddin, M. Grätzel and E. U. Akkaya, Optimization of distyryl-Bodipy chromophores for efficient panchromatic sensitization in dye sensitized solar cells, *Chem. Sci.*, 2011, **2**, 949–954; (*d*) Y. Ooyama, Y. Hagiwara, T. Mizumo, Y. Harima and J. Ohshita, Synthesis of diphenylamino-carbazole substituted BODIPY dyes and their photovoltaic performance in dye-sensitized solar cells, *RSC Adv.*, 2013, **3**, 18099–18106; (*e*) Y. Kubo, D. Eguchi, A. Matsumoto, R. Nishiyabu, H. Yakushiji, K. Shigaki and M. Kaneko, Boron–dibenzopyrromethene-based organic dyes for application in dye-sensitized solar cells, *J. Mater. Chem. A*, 2014, **2**, 5204–5211; (*f*) M. F. Shah, A. Mirloup, T. H. Chowdhury, A. Sutter, A. S. Hanbazazah, A. Ahmed, J.-J. Lee, M. Abdel-Shakour, N. Leclerc, R. Kaneko and A. Islam, Cross-conjugated BODIPY pigment for highly efficient dye sensitized solar cells, *Sustainable Energy Fuels*, 2020, **4**, 1908–1914.

20 A. Poirel, A. De Nicola and R. Ziessel, Oligothienyl-BODIPYs: Red and Near-Infrared Emitters, *Org. Lett.*, 2012, **14**, 5696–5699.